

X-RAY EMISSION FROM THE SUPERGIANT SHELL IN IC 2574

MIHOKO YUKITA¹ AND DOUGLAS A. SWARTZ²

Submitted to Astrophysical Journal Letters

ABSTRACT

The M81 group member dwarf galaxy IC 2574 hosts a supergiant shell of current and recent star-formation activity surrounding a 1000×500 pc hole in the ambient HI gas distribution. *Chandra X-ray Observatory* imaging observations reveal a luminous, $L_X \sim 6.5 \times 10^{38}$ erg s⁻¹ in the 0.3–8.0 keV band, point-like source within the hole but offset from its center and fainter diffuse emission extending throughout and beyond the hole. The star formation history at the location of the point source indicates a burst of star formation beginning ~ 25 Myr ago and currently weakening and there is a young nearby star cluster, at least 5 Myr old, bracketing the likely age of the X-ray source at between 5 and ~ 25 Myr. The source is thus likely a bright high-mass X-ray binary — either a neutron star or black hole accreting from an early B star undergoing thermal-timescale mass transfer through Roche lobe overflow. The properties of the residual diffuse X-ray emission are consistent with those expected from hot gas associated with the recent star-formation activity in the region.

Subject headings: galaxies: individual (IC 2574) — galaxies: starburst — X-rays: binaries — X-rays: galaxies

1. INTRODUCTION

IC 2574 is a low metallicity (Miller & Hodge 1996; Masegosa et al. 1991; Croxall et al. 2009), gas-rich, dwarf irregular galaxy located 4.0 Mpc distant (Karachentsev et al. 2002, $1''=19$ pc) in the M81 group of galaxies.

The galaxy hosts numerous HI holes and shells (Walter et al. 1998; Walter & Brinks 1999), one of which is located in the most prominent region of current and recent star-formation and is near the outskirts of the galaxy. This 1000×500 pc supergiant shell has been studied intensively at UV (Stewart & Walter 2000), optical (Pasquali et al. 2008; Weisz et al. 2009), mid-infrared (Cannon et al. 2005), and radio wavelengths (Walter et al. 1998; Walter & Brinks 1999). Recent analysis of resolved stars imaged with *Hubble* (Weisz et al. 2009) shows that the most significant episodes of star formation began nearly 100 Myr ago and isolated bursts along the shell periphery are as young as 10 Myr. The ages of the younger star-formation events are consistent with those derived from broadband photometry (e.g., Stewart & Walter 2000; Cannon et al. 2005; Pasquali et al. 2008) and only slightly younger than the estimated dynamical age of the HI shell, 14 Myr (Walter et al. 1998; Walter & Brinks 1999).

Walter et al. (1998) also report analysis of soft X-ray emission from the supergiant shell observed with the *ROSAT* PSPC. They found that the emission was extended beyond the $\sim 28''$ FWHM instrumental point-spread function (PSF) with a surface brightness peak near the center of the HI hole. Based on spectral hardness ratios, Walter et al. (1998) compute a plasma temperature of ~ 0.54 keV, a luminosity of 1.6×10^{38} erg s⁻¹ in the 0.3–2.4 keV range, and an electron density of 0.03 cm⁻³ (assuming a metallicity $Z/Z_\odot = 0.15$ and a spherical

emitting volume of 700 pc diameter).

Here, we analyze higher resolution *Chandra* spectrophotometric imaging observations of the supergiant shell. We show that the bulk of the emission arises from a bright point source located within the HI hole (§ 3) with a mildly-absorbed hard power law spectrum (photon index 1.6) and intrinsic luminosity 6.5×10^{38} erg s⁻¹ in the 0.3–8.0 keV range. There remains residual X-ray emission (§ 4) which can be characterized as a diffuse thermal plasma (temperature 0.5 keV, 0.3–8.0 keV luminosity 2.7×10^{37} erg s⁻¹). The emission extends throughout and beyond the HI hole and is likely the result of the recent star formation activity.

We then determine the mass, age, and extinction towards several young star clusters inside and on the supergiant shell (§ 5) and use this to argue that the bright point source is a high-mass X-ray binary (HMXB) with an early B star companion (§ 6). The residual X-ray emission accounts for no more than $\sim 1\%$ of the mechanical energy produced by massive stars and supernovae in the massive star cluster in the HI hole.

2. X-RAY IMAGE ANALYSIS

IC 2574 was observed with the *Chandra X-ray Observatory* Advanced CCD Imaging Spectrometer (ACIS) on 2000 January 7 (ObsID 792) and again on 2008 June 30 (ObsID 9541). Both observations were of approximately 10 ks duration and are sensitive to on-axis point-like sources as faint as $\sim 1.5 \times 10^{37}$ erg s⁻¹. Here, the earlier observation is analyzed because the HI hole was imaged close to the aimpoint and the back-illuminated S3 CCD used for this observation has higher effective area below 1 keV, where most of the X-ray emission is expected from a hot gas bubble, than the front-illuminated ACIS-I array used for the latter observation. We also note that the observation in 2000 was taken early enough in the mission that the soft response of the ACIS CCDs was not yet compromised by the buildup of material on their Optical Blocking Filters. The observation was made in

¹ Department of Physics & Astronomy, University of Alabama, Tuscaloosa, AL, USA

² Universities Space Research Association, NASA Marshall Space Flight Center, VP62, Huntsville, AL, USA

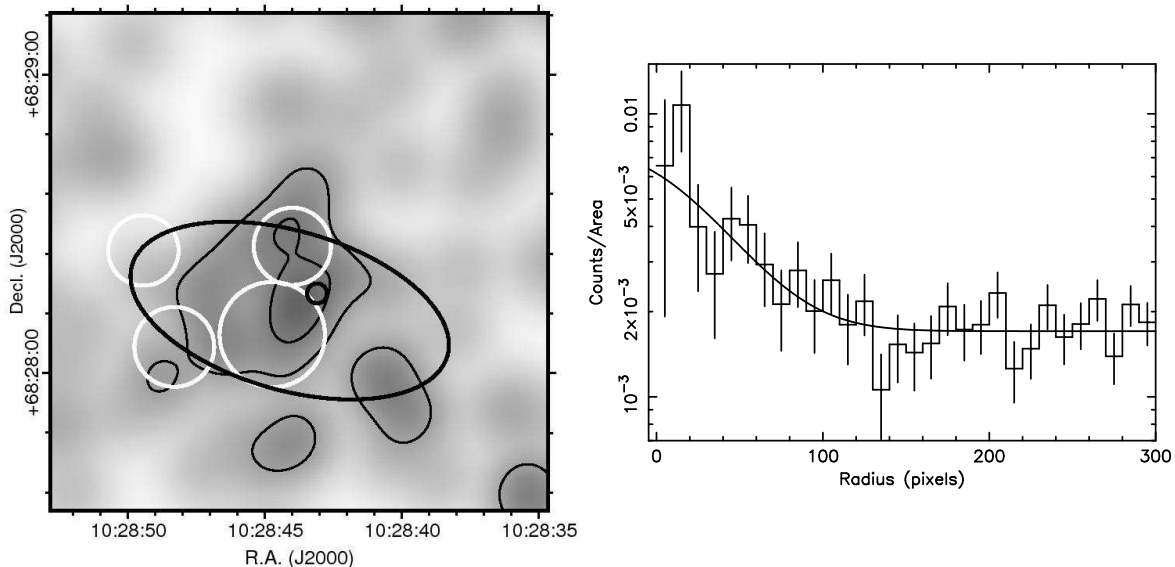


FIG. 1.— Left panel: the diffuse X-ray emission in a $100'' \times 100''$ region of the supergiant shell of IC 2574. The ellipse denotes the HI hole as defined by Walter et al. (1998) and the small circle the position of CXOU J102843.0+682816. The other symbols denote regions identified in Figure 2. The contour levels are at 1 and 2×10^{-9} photon $\text{cm}^{-2} \text{ s}^{-1} \text{ pixel}^{-2}$ (1 pixel = $0''.492$). Right panel: deprojected radial profile of X-ray events (unsmoothed; in the 0.3–2.0 keV energy range). The deprojection assumed that the elliptical HI hole is circular.

the full-frame timed exposure mode using the standard 3.2 s frame time and the VFaint telemetry format.

The data were reprocessed beginning with the Level 1 event list. A time-dependent gain correction was applied and pixel randomization was removed using the *Chandra* X-ray Center’s CIAO ver. 4.3 tool `acis_process_events`. The standard *ASCA* event grades were selected and hot pixels, columns, and cosmic-ray afterglows were removed to create a Level 2 event list for analysis. An ~ 800 s period of high background near the end of the observation was omitted leaving a usable exposure time of ~ 9 ks.

3. CXOU J102843.0+682816

There is a bright X-ray source located inside the supergiant shell. Walter et al. (1998) judged it to be extended based on a *ROSAT* PSPC observation. However, it is clear in the *Chandra* image that most of the X-ray emission is contributed from a single point-like source. An elliptical Gaussian model (plus a constant term) was fit to the spatial distribution of X-ray events in the 0.3–8.0 keV range to determine the source centroid, Gaussian width, and approximate source asymmetry. The best-fitting source position is $10^{\text{h}}28^{\text{m}}43.08^{\text{s}}$, $+68^{\circ}28'16.37''$. The source is symmetrical within measurement errors with an rms Gaussian width of $0.315'' \pm 0.004''$.

A radial profile of the data was compared to a simulation of the PSF built using the *Chandra* Ray Tracer (ChART) and MARX suites of programs available from the *Chandra* X-ray Center. Fitting a Gaussian to the profile of the data and of the simulated PSF (plus a Lorentzian for the wings and a constant for the background) results in a best-fit width of the simulated PSF slightly larger than the observed source width. The source is clearly point-like.

Events were extracted from a $3''$ radius region sur-

rounding the source for spectral analysis. This encircles roughly 99% of the 0.3–8.0 keV flux from the source. A background spectrum was extracted from the surrounding region. An absorbed power law model, including a multiplicative pileup correction, was fit to the background-subtracted spectrum using the XSPEC ver. 11.3.2ag analysis tool.

The best-fitting model column density is $(5.4 \pm 5.8) \times 10^{20} \text{ cm}^{-2}$ which is roughly the Galactic line-of-sight value of $2.2 \times 10^{20} \text{ cm}^{-2}$, the best-fitting power law index is 1.6 ± 0.6 ($\chi^2 = 20.1$ for 31 dof), and the intrinsic X-ray luminosity is $(6.5 \pm 1.5) \times 10^{38} \text{ erg s}^{-1}$ after correcting for $\sim 10\%$ pileup. A thermal plasma model also provides an acceptable fit to the point source spectrum but the resulting temperature, $kT_e \sim 5$ to 18 keV, and X-ray luminosity are much too high to be representative of a hot gas phase associated with star formation.

4. DIFFUSE X-RAY EMISSION

There remains an excess of X-ray events within and around the HI hole ($66'' \times 32''$) after removing CXOU J102843.0+682816 from the image. This soft X-ray diffuse emission has low surface brightness, which leads to a grainy, low S/N, image. The emission can be seen more easily if the image is artificially smoothed. The point source was removed using a $3''$ radius circle, which is large enough to avoid leaving residual emission from the wings of the point source. Then, the excluded region was filled using the local background level Poisson method of the CIAO tool `dmfilth`. The filled image was then divided by a 0.5 keV monochromatic exposure map, then smoothed with the CIAO tool `aconvolve` using a Gaussian smoothing function with a width of 10 pixels ($\sim 5''$).

The left panel of Figure 1 shows the smoothed soft X-ray diffuse map of a $100'' \times 100''$ region around the su-

TABLE 1
PROPERTIES OF STAR-FORMING REGIONS

Region	Age (Myr)	Mass ($10^5 M_\odot$)	A_V (mag)	L_W (10^{38} erg s $^{-1}$)	Net Counts	L_X^{int} (10^{35} erg s $^{-1}$)
C1	7	0.8	0.0	27	6.8±2.8	38±16
C2	17	1.5	0.0	29	9.3±3.3	52±19
C3	17	0.9	0.1	16	1.0±1.4	6±8
C4	7	0.2	0.1	4.7	-0.4±1.0	-2±6

pergiant shell. The HI hole is denoted by an ellipse and the location of CXOU J102843.0+682816 by a small circle. There is a net of 28.1 ± 5.3 X-ray events in the energy range of 0.3–8.0 keV inside the HI hole after subtracting background. (The background was defined as emission in the S3 chip outside the optical extent of IC 2574, defined by an ellipse approximating the 25 mag s $^{-1}$ blue light isophote, after excluding any detected point sources.) We note that 90% of the emission is found in the soft band (0.3–2.0 keV).

The right panel of Figure 1 displays the radial profile of events in the 0.3–2.0 keV energy range of the diffuse emission after deprojecting the image. The deprojection was made assuming that the $66'' \times 32''$ elliptical HI hole is actually circular. The radial profile is centered on the HI hole center. It clearly shows the excess emission within the HI hole and perhaps extending slightly beyond the hole. Note that there is no emission enhancement within the current star-forming regions in the shell surrounding the hole. The broad energy distribution of the X-ray events within the HI hole was compared to a grid of models of an absorbed thermal plasma. Specifically, the ratios of observed events in the 0.3–1.0 to 0.3–8.0 and in the 0.3–1.0 to 0.3–2.0 bands most closely match a model of temperature 0.5 ± 0.1 keV and intervening absorption column of $(4 \pm 2) \times 10^{20}$ cm $^{-2}$ where the errors denote the model grid spacing. This model results in a luminosity of $(2.7 \pm 0.5) \times 10^{37}$ erg s $^{-1}$ in the 0.3–8.0 keV range where the error is based on the net source counts.

5. MASS, AGE, AND EXTINCTION IN SUPERGIANT SHELL STAR-FORMING REGIONS

As mentioned in the introduction, several previous studies have provided estimates of the mass and/or age of star-forming regions associated with the supergiant shell. We have performed our own multi-wavelength analysis which produces self-consistent age, mass, and extinction estimates for individual (assumed co-eval) star clusters. The method is presented in detail in Yukita (2010).

Briefly, the analysis uses the Starburst99 stellar synthesis program (Leitherer et al. 1999) to compute star cluster model spectra as a parameterized function of cluster age, star formation history, and metallicity from a combination of stellar evolution tracks and a grid of stellar model atmospheres weighted by an initial mass function (IMF). We assume a (single) instantaneous burst history, solar metallicity, and a Salpeter IMF (Salpeter 1955). Transmission of the composite stellar spectra through the surrounding ISM is modeled using a standard starburst dust extinction model (Calzetti et al. 2000) that modifies the blue portion of the spectrum and we assume that the dust re-emits this radiation as a blackbody (fixed at $T = 30$ K, see Cannon et al. 2005)

in the IR band. Finally, the (dust-modified) emergent model spectra are convolved with instrumental response functions appropriate to the various instruments and the best-fitting solution to the observed broadband photometry is determined. (The observations are corrected for a line-of-sight Galactic extinction of $A_V = 0.120$ (Schlegel et al. 1998) using the Cardelli et al. (1989) dust model.) This method self-consistently overcomes the age-extinction degeneracy when fitting models to UV-to-IR broadband photometry.

Here, we use calibrated GALEX FUV and NUV observations available through the *GalexView* data interface³ and *Spitzer* 3.6, 4.5, and 24 μ m observations processed and made available as part of the *Spitzer* Infrared Nearby Galaxies Survey (Kennicutt et al. 2003). Images of the supergiant shell at several passbands are displayed in Figure 2. A continuum-subtracted H α image observed with the Kitt Peak 2.1 m telescope using the T2KB CCD Imager in 2008 March (1.3'' seeing) is also shown.

Our cluster selection is to be both FUV and 24 μ m bright sources. Three clusters around the shell were identified from both FUV and 24 μ m images. The UV bright cluster located in the HI hole has been well studied (Stewart & Walter 2000; Pasquali et al. 2008) therefore it is also investigated further, although it lacks 24 μ m emission. Overall, the total of four isolated star clusters were analyzed. These are marked in the figure along with the position of CXOU J102843.0+682816 and the elliptical boundary of the HI hole. The best-fit age, mass, and extinction derived for these clusters are listed in Table 1. Also listed are the current mechanical luminosities from stellar winds and supernovae, L_W , corresponding to the best-fitting Starburst99 model, X-ray background-subtracted net counts in circular apertures of size equal to the 99% FUV encircled energy region in the 0.5–2.0 keV energy range, and the corresponding X-ray luminosity, L_X , in the 0.5–2.0 keV energy range assuming a 0.5 keV thermal plasma X-ray spectral shape.

All clusters are young and the masses of the clusters are on the order of $10^4 M_\odot$ with the exception of C2. C2 is the central stellar cluster located within the HI hole surrounded by the supergiant shell. The age of this cluster has been estimated as 11 Myr from the FUV observation (Stewart & Walter 2000) and 5 Myr from the optical data (Pasquali et al. 2008). We obtain a slightly older age. Stewart & Walter (2000) also estimate the mass of the cluster as $1.4 \times 10^5 M_\odot$ consistent with the present result of $1.5 \times 10^5 M_\odot$. Both authors also found that the HII regions in the vicinity of the cluster are younger, having ages of 1–3 Myr, which is less than the present results. (We note that we obtain ages of 2–3 Myr if we assume a

³ <http://galex.stsci.edu/GalexView/>

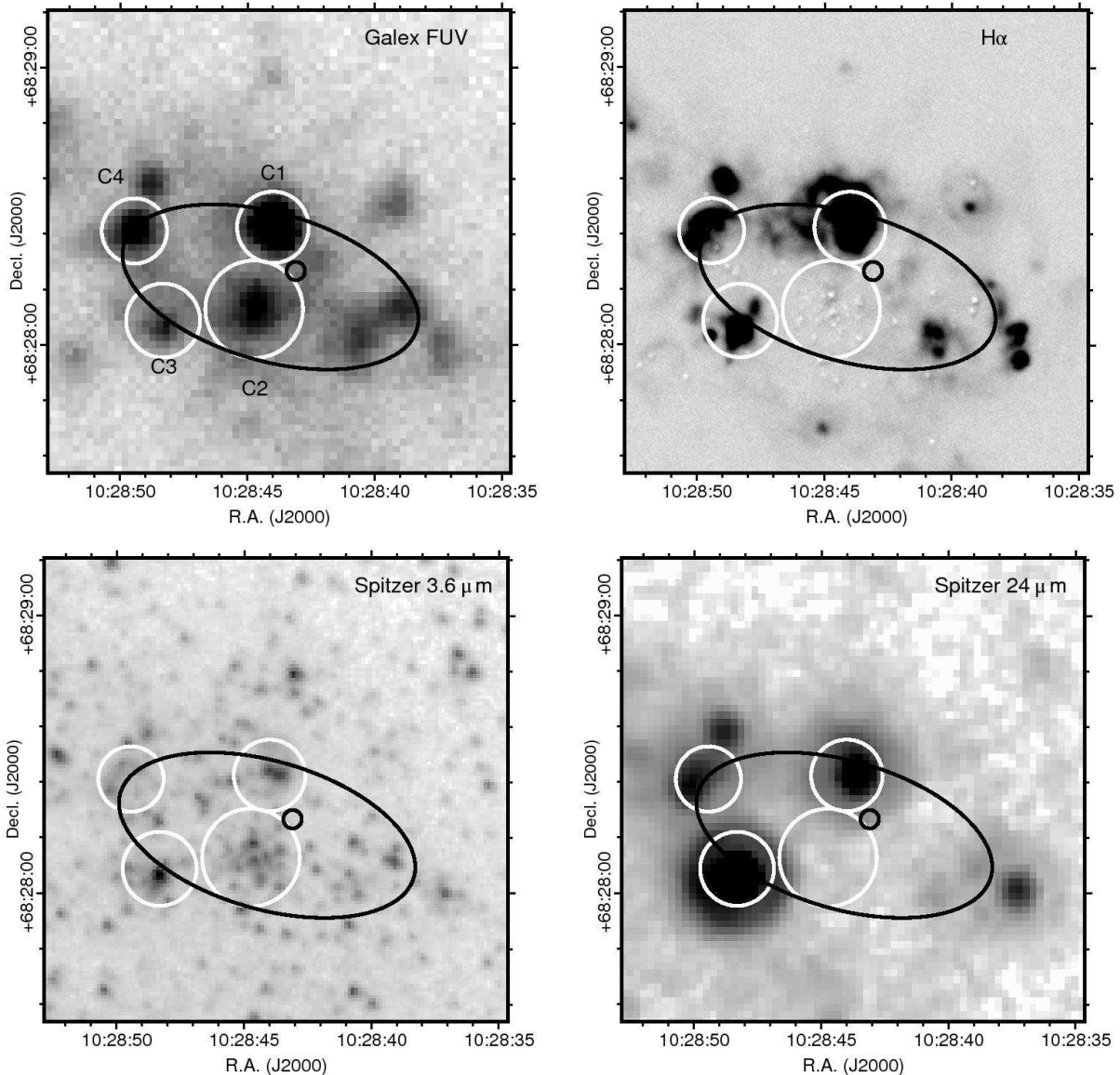


FIG. 2.— Clockwise from top left: FUV, $H\alpha$, $24\ \mu\text{m}$, and $3.6\ \mu\text{m}$ images of the same supergiant shell region as depicted in Figure 1. Four star clusters identified in the $24\ \mu\text{m}$ and FUV are denoted by white circles depicting 3σ aperture sizes defined by circular Gaussian fits to the FUV data.

canonical dust temperature of 70 K.) This age gradient supports the premise of propagating star formation such that the mechanical energy from the central cluster compresses the surrounding ISM and triggers subsequent star formation at the rim. The mass of C2 is large enough to drive star formation in the surroundings: The derived mechanical luminosity for C2 is $2.9 \times 10^{39}\ \text{erg s}^{-1}$. The cumulative energy released is 2×10^{54} erg over the lifetime of the cluster, which is much more than needed to create the hole (2×10^{53} erg; Walter et al. 1998).

6. SUMMARY AND DISCUSSION

High-angular resolution *Chandra* spectrophotometric imaging of the HI hole and surrounding supergiant shell in IC 2574 reveal a bright point source, CXOU J102843.0+682816, near the center of the HI hole and residual low surface brightness soft X-ray

emission throughout the hole and in the surrounding shell. Analysis of the UV-to-IR spectral energy distributions of several representative star clusters in and around the HI hole results in age and mass estimates consistent with previous studies. In particular, there is a massive, $1.5 \times 10^5 M_{\odot}$, intermediate-age, 5–17 Myr, cluster near the center of the hole that has released enough mechanical energy from massive stars and supernovae over its lifetime to have created the hole. Our analysis is consistent with previous analyses of the supergiant shell in IC 2574 (Walter et al. 1998; Walter & Brinks 1999; Stewart & Walter 2000; Pasquali et al. 2008; Weisz et al. 2009) and supports the classical picture of bubble formation and evolution such that younger star clusters on the periphery of the hole likely formed as a consequence of this stellar feedback sweeping ambient material into dense

clouds that collapse under self-gravity and subsequently form new stars (e.g., Larson 1974; Weaver et al. 1977; McCray & Kafatos 1987; Mac Low & McCray 1988).

We have shown that the ratio of X-ray to mechanical luminosity in these young star clusters in the region is $\lesssim 0.2\%$. Observed ratios of 0.1% to 1% are typical of many star-forming regions (Yukita 2010) but are poorly constrained theoretically because of uncertainties in ambient conditions, starburst histories, and three-dimensional geometries. For example, we note that the central cluster alone could be responsible for all the X-ray diffuse emission within the HI hole; the mechanical luminosity from the central cluster is 2.9×10^{39} erg s $^{-1}$ and the diffuse X-ray luminosity from the hole is 2.7×10^{37} erg s $^{-1}$. Weisz et al. (2009) estimate that the cumulative energy released from the whole region in the past ~ 25 Myr is $\sim 10^{55}$ erg. Even at a constant (current) rate, less than 0.1% of the total energy from stars has been lost to the X-ray radiation. Thus, the central cluster in the HI hole alone can account for the diffuse X-ray emission and the creation of the HI hole. Perhaps we are witnessing powerful positive feedback from this central cluster in the form of subsequent star formation in the surrounding supergiant shell.

Most of the X-ray emission in the HI hole in IC 2574 comes from the single bright source CXOU J102843.0+682816. The presence of such a luminous X-ray point source in even a massive supergiant shell is uncommon. Recent supernovae can be this luminous but they, too, are rare and typically much softer than CXOU J102843.0+682816. The high luminosity, hard spectral shape, and large numbers of recently-formed stars in the vicinity suggest that CXOU J102843.0+682816 is an HMXB. We can esti-

mate the age of the binary system at between 5 Myr, the youngest age of the nearby massive star cluster, and 25 Myr, the age of the peak in the star-formation rate at the location of CXOU J102843.0+682816 as determined by Weisz et al. (2009). The compact object must then have had a minimum initial mass between about 10 and 40 M_{\odot} to have already evolved to a supernova endpoint. The companion is likely also of roughly this mass in order to provide the required high mass accretion rate. This rate can be estimated assuming $L_X \sim L_{\text{bol}} \sim \eta \dot{m} c^2$ with an efficiency, $\eta \sim 0.1$, giving $\dot{m} \sim 10^{-7} M_{\odot} \text{ yr}^{-1}$. According to Podsiadlowski et al. (2003), this requires a companion star mass of at least 8–10 M_{\odot} and higher if the system is older, if the bolometric luminosity exceeds the X-ray luminosity, or if mass is lost from the system. Podsiadlowski et al. (2003) also estimate the rate of formation of systems of this type scaled to a fiducial supernova rate. Their rate can be converted to a total number of systems in the central star cluster as there are about one $M > 8 M_{\odot}$ star (i.e., stars that eventually undergo supernovae) per 50 M_{\odot} of star formation for a Salpeter IMF. Thus, the Podsiadlowski et al. (2003) rate of $< 10^{-4} \text{ yr}^{-1}$ per 8 M_{\odot} star translates to 0.3 luminous HMXBs for the central star cluster of mass $1.5 \times 10^5 M_{\odot}$. This is a high estimate because not all the potential compact objects have yet been created by supernova events. Thus, objects like CXOU J102843.0+682816 are indeed rare even for massive star clusters.

We gratefully acknowledge the referee, Leisa Townsley, for her expert critique and especially for alerting us to the possibility of pile-up of the point source. Support for this research was provided in part by NASA through an Astrophysics Data Analysis Program grant NNX08AJ49G.

REFERENCES

- Calzetti, D., Armus, L., Bohlin, R. C., Kinney, A. L., Koornneef, J., & Storchi-Bergmann, T. 2000, *ApJ*, 533, 682
 Cannon, J. M., et al. 2005, *ApJ*, 630, L37
 Cardelli, J. A., Clayton, G. C., & Mathis, J. S. 1989, *ApJ*, 345, 245
 Croxall, K. V., van Zee, L., Lee, H., Skillman, E. D., Lee, J. C., Côté, S., Kennicutt, R. C., & Miller, B. W. 2009, *ApJ*, 705, 723
 Karachentsev, I. D., et al. 2002, *A&A*, 383, 125
 Kennicutt, Jr., R. C., et al. 2003, *PASP*, 115, 928
 Larson, R. B. 1974, *MNRAS*, 169, 229
 Leitherer, C., et al. 1999, *ApJS*, 123, 3
 Mac Low, M.-M., & McCray, R. 1988, *ApJ*, 324, 776
 Masegosa, J., Moles, M., & del Olmo, A. 1991, *A&A*, 249, 505
 McCray, R., & Kafatos, M. 1987, *ApJ*, 317, 190
 Miller, B. W., & Hodge, P. 1996, *ApJ*, 458, 467
 Pasquali, A., et al. 2008, *ApJ*, 687, 1004
 Podsiadlowski, P., Rappaport, S., & Han, Z. 2003, *MNRAS*, 341, 385
 Salpeter, E. E. 1955, *ApJ*, 121, 161
 Schlegel, D. J., Finkbeiner, D. P., & Davis, M. 1998, *ApJ*, 500, 525
 Stewart, S. G., & Walter, F. 2000, *AJ*, 120, 1794
 Walter, F., & Brinks, E. 1999, *AJ*, 118, 273
 Walter, F., Kerp, J., Duric, N., Brinks, E., & Klein, U. 1998, *ApJ*, 502, L143+
 Weaver, R., McCray, R., Castor, J., Shapiro, P., & Moore, R. 1977, *ApJ*, 218, 377
 Weisz, D. R., Skillman, E. D., Cannon, J. M., Walter, F., Brinks, E., Ott, J., & Dolphin, A. E. 2009, *ApJ*, 691, L59
 Yukita, M. 2010, PhD thesis, The University of Alabama in Huntsville